

PAPER • OPEN ACCESS

The Advanced Virgo+ status

To cite this article: F Acernese *et al* 2023 *J. Phys.: Conf. Ser.* **2429** 012039

View the [article online](#) for updates and enhancements.

You may also like

- [Fast \$b\$ -tagging at the high-level trigger of the ATLAS experiment in LHC Run 3](#)
G. Aad, B. Abbott, K. Abeling *et al.*
- [The ATLAS Fast Tracker system](#)
The ATLAS collaboration, G. Aad, B. Abbott *et al.*

The Advanced Virgo+ status

F Acernese^{1,2}, M Agathos³, A Ain⁴, S Albanesi^{5,6}, C Alléné⁷,
 A Allocca^{8,2}, A Amato^{9,10}, M Andia¹¹, T Andrade¹², N Andres⁷,
 M Andrés-Carcasona¹³, T Andrić¹⁴, S Ansoldi^{15,16}, S Antier¹⁷,
 T Apostolatos¹⁸, E Z Appavuravther^{19,20}, M Arène²¹, N Arnaud^{11,22},
 M Assiduo^{23,24}, S Assis de Souza Melo²², P Astone²⁵, F Aubin²⁴,
 S Babak²¹, F Badaracco²⁶, S Bagnasco⁶, J Baird²¹, T Baka²⁷,
 G Ballardín²², G Baltus²⁸, B Banerjee¹⁴, P Barneo^{12,29},
 F Barone^{30,2}, M Barsuglia²¹, D Barta³¹, A Basti^{32,4},
 M Bawaj^{33,19}, M Bazzan^{34,35}, F Beirnaert³⁶, M Beijger³⁷,
 V Benedetto³⁸, M Berbel³⁹, S Bernuzzi³, D Bersanetti⁴⁰,
 A Bertolini¹⁰, U Bhardwaj^{41,10}, A Bianchi^{10,42}, M Bilicki⁴³,
 S Bini^{44,45}, M Bischì^{23,24}, M Bitossi^{22,4}, M-A Bizouard¹⁷,
 F Bobba^{46,47}, M Boër¹⁷, G Bogaert¹⁷, G . Boileau^{48,17},
 M Boldrini^{49,25}, L D Bonavena³⁴, R Bondarescu¹², F Bondu⁵⁰,
 R Bonnand⁷, V Boschi⁴, V Boudart²⁸, Y Bouffanais^{34,35},
 A Bozzi²², C Bradaschia⁴, M Braglia⁵¹, M Branchesi^{14,52},
 M Breschi³, T Briant⁵³, A Brillet¹⁷, J Brooks²², G Bruno²⁶,
 F Bucci²⁴, O Bulashenko^{12,29}, T Bulik⁵⁴, H J Bulten¹⁰,
 R Buscicchio^{55,56}, D Buskulić⁷, C Buy⁵⁷, G Cabras^{15,16},
 R Cabrita²⁶, G Cagnoli⁵⁸, E Calloni^{8,2}, M Canepa^{59,40},
 G Caneva¹³, M Cannavacciuolo⁴⁶, E Capocasa²¹, G Carapella^{46,47},
 F Carbognani²², M Carpinelli^{55,60,22}, G Carullo^{32,4},
 J Casanueva Diaz²², C Casentini^{61,62}, S Caudill^{10,27}, R Cavalieri²²,
 G Cella⁴, P Cerdá-Durán⁶³, E Cesarini⁶², W Chaibi¹⁷,
 P Chaniá^{22,21}, E Chassande-Mottin²¹, S Chaty²¹, P Chessa^{32,4},
 F Chiadini^{64,47}, G Chiarini³⁵, R Chierici⁶⁵, A Chincarini⁴⁰,
 M L Chiofalo^{32,4}, A Chiummo²², N Christensen¹⁷, G Ciani^{34,35},
 P Ciecielag³⁷, M Cieřlar³⁷, M Cifaldi^{61,62}, R Ciolfi^{66,35}, S Clesse⁶⁷,
 F Cleva¹⁷, E Coccia^{14,52}, E Codazzo¹⁴, P-F Cohadon⁵³,
 A Colombo^{55,56}, M Colpi^{55,56}, L Conti³⁵, I Cordero-Carrión⁶⁸,
 S Corezzi^{33,19}, S Cortese²², J-P Coulon¹⁷, J-F Coupechoux⁶⁵,
 M Croquette⁵³, J R Cudell²⁸, E Cuoco^{22,69,4}, M Curyłó⁵⁴,
 P Dabadie⁵⁸, T Dal Canton¹¹, S Dall’Osso²⁵, G Dálya³⁶,
 B D’Angelo^{59,40}, S Danilishin^{9,10}, S D’Antonio⁶², V Dattilo²²,
 M Davier¹¹, J Degallaix⁷³, M De Laurentis^{8,2}, S Deléglise⁵³,
 F De Lillo²⁶, D Dell’Aquila^{70,60}, W Del Pozzo^{32,4}, F De Matteis^{61,62},
 A Depasse²⁶, R De Pietri^{71,72}, R De Rosa^{8,2}, C De Rossi²²,
 R De Simone⁶⁴, L Di Fiore², C Di Giorgio^{46,47}, F Di Giovanni⁶³,
 M Di Giovanni¹⁴, T Di Girolamo^{8,2}, D Diksha^{10,9}, A Di Lieto^{32,4},
 A Di Michele³³, S Di Pace^{49,25}, I Di Palma^{49,25}, F Di Renzo^{22,4},



L D'Onofrio^{8,2}, T Dooney²⁷, O Dorosh⁷⁴, M Drago^{49,25},
 J-G Ducoin^{75,21}, U Dupletsa¹⁴, O Durante^{46,47}, D D'Urso^{70,60},
 P-A Duverne¹¹, L Errico^{8,2}, D Estevez⁷⁶, F Fabrizi^{23,24}, F Faedi²⁴,
 V Fafone^{61,62,14}, G Favaro³⁴, M Fays²⁸, E Fenyvesi^{31,77},
 I Ferrante^{32,4}, F Fidecaro^{32,4}, P Figura⁵⁴, A Fiori^{4,32}, I Fiori²²,
 R Fittipaldi^{78,47}, V Fiumara^{79,47}, R Flaminio^{7,80}, J A Font^{63,81},
 S Frasca^{49,25}, F Frasconi⁴, A Freise^{10,42}, O Freitas⁸², G G Fronzé⁶,
 B Gadre²⁷, R Gamba³, B Garaventa^{40,59}, J Garcia-Bellido⁵¹,
 J Gargiulo²², F Garufi^{8,2}, C Gasbarra^{61,62}, G Gemme⁴⁰,
 A Gennai⁴, Archisman Ghosh³⁶, L Giacoppo^{49,25}, P Giri^{4,32},
 F Gissi³⁸, S Gkaitatzis²², F Glotin¹¹, B Goncharov¹⁴, M Gosselin²²,
 R Gouaty⁷, A Grado^{83,2}, M Granata⁷³, V Granata⁴⁶, G Greco¹⁹,
 G Grignani^{33,19}, A Grimaldi^{44,45}, D Guerra⁶³, D Guetta²⁵,
 G M Guidi^{23,24}, F Gulminelli^{84,85}, Y Guo¹⁰, P Gupta^{10,27},
 N Gutierrez⁷³, L Haegel²¹, O Halim¹⁶, O Hannuksela^{27,10},
 T Harder¹⁷, K Haris^{10,27}, T Harmark⁸⁶, J Harms^{14,52}, B Haskell³⁷,
 A Heidmann⁵³, H Heitmann¹⁷, P Hello¹¹, G Hemming²²,
 E Hennes¹⁰, J-S Hennig^{9,10}, M Hennig^{9,10}, S Hild^{9,10}, D Hofman⁷³,
 N A Holland^{10,42}, V Hui⁷, G A Iandolo⁹, B Idzkowski⁵⁴,
 A Iess^{69,4}, G Iorio³⁴, P Iosif⁸⁷, T Jacqmin⁵³, P-E Jacquet⁵³,
 J Janquart^{27,10}, K Janssens^{48,17}, S Jaraba⁵¹, P Jaranowski⁸⁸,
 P Jasal¹², V Juste⁷⁶, C Kalaghatgi^{27,10,89}, C Karathanasis¹³,
 S Katsanevas²², F Kéfélian¹⁷, G Koekoek^{10,9}, S Koley¹⁴,
 M Kolstein¹³, S L Kranzhoff^{9,10}, A Królak^{90,74}, P Kuijer¹⁰,
 S Kuroyanagi⁵¹, P Lagabbe⁷, D Laghi⁵⁷, M Lalleman⁴⁸,
 A Lamberts^{17,91}, A La Rana²⁵, I La Rosa⁷, A Lartaux-Vollard¹¹,
 C Lazzaro^{34,35}, P Leaci^{49,25}, A Lemaître⁹², M Lenti^{24,93},
 E Leonova⁴¹, N Leroy¹¹, N Letendre⁷, M Lethuillier⁶⁵, K Leyde²¹,
 F Linde^{89,10}, L London⁴¹, A Longo⁹⁴, M Lopez Portilla²⁷,
 M Lorenzini^{61,62}, V Loriette⁹⁵, G Losurdo⁴, D Lumaca^{61,62},
 A Macquet^{13,17}, C Magazzù⁴, R Maggiore^{10,42}, M Magnozzi^{40,59},
 E Majorana^{49,25}, N Man¹⁷, V Mangano^{49,25}, M Mantovani²²,
 M Mapelli^{34,35}, F Marchesoni^{20,19,96}, D Marín Pina^{12,29,97},
 F Marion⁷, A Marquina⁶⁸, S Marsat⁵⁷, F Martelli^{23,24},
 M Martinez¹³, V Martinez⁵⁸, A Masserot⁷, M Mastrodicasa²⁵,
 S Mastrogiovanni¹⁷, Q Meijer²⁷, A Menendez-Vazquez¹³,
 L Mereni⁷³, M Merzougui¹⁷, A Miani^{44,45}, C Michel⁷³, A Miller²⁶,
 B Miller^{41,10}, E Milotti^{98,16}, Y Minenkov⁶², Ll. M Mir¹³,
 M Miravet-Tenés⁶³, A L Mitchell^{10,42}, C Mondal⁸⁴, M Montani^{23,24},
 F Morawski³⁷, G Morras⁵¹, B Mours⁷⁶, C M Mow-Lowry^{10,42},
 F Muciaccia^{49,25}, Suvodip Mukherjee⁴¹, A Nagar^{6,99}, V Napolano²²,
 I Nardecchia^{61,62}, H Narola²⁷, L Naticchioni²⁵, J Neilson^{38,47},
 S Nesseris⁵¹, C Nguyen²¹, G Nieradka³⁷, S Nissanke^{41,10},
 E Nitoglia⁶⁵, F Nocera²², J Novak^{100,101,102,103}, J F Nuño Siles⁵¹,
 M Oertel^{100,101,102,104,103}, G Oganessian^{14,52}, R Oliveri^{100,101,102},
 M Orselli^{19,33}, C Palomba²⁵, P T H Pang^{10,27}, F Pannarale^{49,25},
 F Paoletti⁴, A Paoli²², A Paolone^{25,105}, G Pappas⁸⁷, A Parisi^{4,69},
 D Pascucci³⁶, A Pasqualetti²², R Passaquieti^{32,4}, D Passuello⁴,
 B Patricelli^{32,4}, R Pedurand⁴⁷, R Pegna^{4,32}, M Pegoraro³⁵,
 A Perego^{44,45}, A Pereira⁵⁸, C Périgois⁶⁶, A Perreca^{44,45}, S Perriès⁶⁵,

J W Perry^{10,42}, D Pesios⁸⁷, C Petrillo³³, K S Phukon^{10,89},
 O J Piccinni^{25,13}, M Pichot¹⁷, M Piendibene^{32,4}, F Piergiovanni^{23,24},
 L Pierini^{49,25}, G Pierra⁶⁵, V Pierro^{38,47}, G Pillant²², M Pillas¹¹,
 F Pilo⁴, L Pinard⁷³, I M Pinto^{38,47,106,8}, M Pinto²²,
 K Piotrkowski²⁶, A Placidi^{19,33}, E Placidi^{49,25}, W Plastino^{107,94},
 R Poggiani^{32,4}, E Polini⁷, E Porcelli¹⁰, J Portell^{12,29,97},
 E K Porter²¹, R Poulton²², M Pracchia⁷, T Pradier⁷⁶,
 M Principe^{38,106,47}, G A Prodi^{108,45}, P Proposito^{61,62}, A Puecher^{10,27},
 M Punturo¹⁹, F Puosi^{4,32}, P Puppo²⁵, G Raaijmakers^{41,10},
 N Radulesco¹⁷, P Rapagnani^{49,25}, M Razzano^{32,4}, T Regimbau⁷,
 L Rei⁴⁰, P Rettegno^{5,6}, B Revenu^{21,109}, A Reza¹⁰, A S Rezaei^{25,49},
 F Ricci^{49,25}, S Rinaldi^{32,4}, F Robinet¹¹, A Rocchi⁶², L Rolland⁷,
 M Romanelli⁵⁰, R Romano^{1,2}, A Romero¹³, S Ronchini^{14,52},
 L Rosa^{2,8}, D Rosińska⁵⁴, S Roy²⁷, D Rozza^{70,60}, P Ruggi²²,
 E Ruiz Morales⁵¹, P Saffarieh^{10,42}, O S Salafia^{55,56,110}, L Salconi²²,
 F Salemi^{44,45}, M Sallé¹⁰, A Samajdar⁵⁶, N Sanchis-Gual^{111,63},
 A Sanuy¹², A Sasli⁸⁷, P Sassi^{19,33}, B Sassolas⁷³, S Sayah⁷³,
 S Schmidt²⁷, M Seglar-Arroyo⁷, D Sentenac²², V Sequino^{8,2},
 G Servignat¹⁰¹, Y Setyawati²⁷, N S Shcheblanov^{112,92},
 M Sieniawska²⁶, L Silenzi^{19,20}, N Singh⁵⁴, A Singha^{9,10},
 V Sipala^{70,60}, J Soldateschi^{93,113,24}, V Sordini⁶⁵, F Sorrentino⁴⁰,
 N Sorrentino^{32,4}, R Soulard¹⁷, V Spagnuolo^{9,10}, M Spera^{34,35},
 P Spinicelli²², C Stachie¹⁷, D A Steer²¹, J Steinlechner^{9,10},
 S Steinlechner^{9,10}, N Stergioulas⁸⁷, G Stratta^{114,25}, M Suchenek³⁷,
 A Sur³⁷, J Suresh²⁶, B L Swinkels¹⁰, A Syx⁷⁶, P Szweczyk⁵⁴,
 M Tacca¹⁰, N Tamanini⁵⁷, A J Tanasijczuk²⁶,
 E N Tapia San Martín¹⁰, C Taranto⁶¹, M Tonelli^{32,4},
 A Torres-Forné⁶³, I Tosta e Melo⁶⁰, E Tournefier⁷,
 A Trapananti^{20,19}, F Travasso^{20,19}, J Trenado¹², M C Tringali²²,
 L Troiano^{115,47}, A Trovato^{16,98}, L Trozzo², K W Tsang^{10,116,27},
 K Turbang^{117,48}, M Turconi¹⁷, C Turski³⁶, H Ubach^{12,29},
 A Utina^{9,10}, M Valentini^{44,45}, S Vallero⁶, N van Bakel¹⁰,
 M van Beuzekom¹⁰, M van Dael^{10,118}, J F J van den Brand^{9,42,10},
 C Van Den Broeck^{27,10}, M van der Sluys^{10,27}, A Van de Walle¹¹,
 J van Dongen^{10,42}, H van Haevermaet⁴⁸, J V van Heijningen²⁶,
 Z van Ranst⁹, N van Remortel⁴⁸, M Vardaro^{89,10}, M Vasúth³¹,
 G Vedovato³⁵, P Verdier⁶⁵, D Verkindt⁷, P Verma⁷⁴, F Vetrano²³,
 A Viceré^{23,24}, J-Y Vinet¹⁷, S Viret⁶⁵, A Virtuoso^{98,16}, H Vocca^{33,19},
 R C Walet¹⁰, M Was⁷, N Yadav³⁷, A Zdrożny⁷⁴, T Zelenova²²,
 and J-P Zendri³⁵

¹Dipartimento di Farmacia, Università di Salerno, I-84084 Fisciano, Salerno, Italy

²INFN, Sezione di Napoli, I-80126 Napoli, Italy

³Theoretisch-Physikalisches Institut, Friedrich-Schiller-Universität Jena, D-07743 Jena, Germany

⁴INFN, Sezione di Pisa, I-56127 Pisa, Italy

⁵Dipartimento di Fisica, Università degli Studi di Torino, I-10125 Torino, Italy

⁶INFN Sezione di Torino, I-10125 Torino, Italy

⁷Univ. Savoie Mont Blanc, CNRS, Laboratoire d'Annecy de Physique des Particules - IN2P3, F-74000 Annecy, France

⁸Università di Napoli "Federico II", I-80126 Napoli, Italy

⁹Maastricht University, 6200 MD Maastricht, Netherlands

¹⁰Nikhef, 1098 XG Amsterdam, Netherlands

- ¹¹Université Paris-Saclay, CNRS/IN2P3, IJCLab, 91405 Orsay, France
- ¹²Institut de Ciències del Cosmos (ICCUB), Universitat de Barcelona (UB), c. Martí i Franquès, 1, 08028 Barcelona, Spain
- ¹³Institut de Física d'Altes Energies (IFAE), Barcelona Institute of Science and Technology, and ICREA, E-08193 Barcelona, Spain
- ¹⁴Gran Sasso Science Institute (GSSI), I-67100 L'Aquila, Italy
- ¹⁵Dipartimento di Scienze Matematiche, Informatiche e Fisiche, Università di Udine, I-33100 Udine, Italy
- ¹⁶INFN, Sezione di Trieste, I-34127 Trieste, Italy
- ¹⁷Université Côte d'Azur, Observatoire Côte d'Azur, CNRS, Artemis, F-06304 Nice, France
- ¹⁸Department of Physics, National and Kapodistrian University of Athens, 15771 Ilissia, Greece
- ¹⁹INFN, Sezione di Perugia, I-06123 Perugia, Italy
- ²⁰Università di Camerino, I-62032 Camerino, Italy
- ²¹Université Paris Cité, CNRS, Astroparticule et Cosmologie, F-75013 Paris, France
- ²²European Gravitational Observatory (EGO), I-56021 Cascina, Pisa, Italy
- ²³Università degli Studi di Urbino "Carlo Bo", I-61029 Urbino, Italy
- ²⁴INFN, Sezione di Firenze, I-50019 Sesto Fiorentino, Firenze, Italy
- ²⁵INFN, Sezione di Roma, I-00185 Roma, Italy
- ²⁶Université catholique de Louvain, B-1348 Louvain-la-Neuve, Belgium
- ²⁷Institute for Gravitational and Subatomic Physics (GRASP), Utrecht University, 3584 CC Utrecht, Netherlands
- ²⁸Université de Liège, B-4000 Liège, Belgium
- ²⁹Departament de Física Quàntica i Astrofísica (FQA), Universitat de Barcelona (UB), c. Martí i Franquès, 1, 08028 Barcelona, Spain
- ³⁰Dipartimento di Medicina, Chirurgia e Odontoiatria "Scuola Medica Salernitana", Università di Salerno, I-84081 Baronissi, Salerno, Italy
- ³¹Wigner RCP, RMKI, H-1121 Budapest, Hungary
- ³²Università di Pisa, I-56127 Pisa, Italy
- ³³Università di Perugia, I-06123 Perugia, Italy
- ³⁴Università di Padova, Dipartimento di Fisica e Astronomia, I-35131 Padova, Italy
- ³⁵INFN, Sezione di Padova, I-35131 Padova, Italy
- ³⁶Universiteit Gent, B-9000 Gent, Belgium
- ³⁷Nicolaus Copernicus Astronomical Center, Polish Academy of Sciences, 00-716, Warsaw, Poland
- ³⁸Dipartimento di Ingegneria, Università del Sannio, I-82100 Benevento, Italy
- ³⁹Departamento de Matemáticas, Universitat Autònoma de Barcelona, 08193 Bellaterra (Barcelona), Spain
- ⁴⁰INFN, Sezione di Genova, I-16146 Genova, Italy
- ⁴¹GRAPPA, Anton Pannekoek Institute for Astronomy and Institute for High-Energy Physics, University of Amsterdam, 1098 XH Amsterdam, Netherlands
- ⁴²Department of Physics and Astronomy, Vrije Universiteit Amsterdam, 1081 HV Amsterdam, Netherlands
- ⁴³Center for Theoretical Physics, Polish Academy of Sciences, 02-668, Warsaw, Poland
- ⁴⁴Università di Trento, Dipartimento di Fisica, I-38123 Povo, Trento, Italy
- ⁴⁵INFN, Trento Institute for Fundamental Physics and Applications, I-38123 Povo, Trento, Italy
- ⁴⁶Dipartimento di Fisica "E.R. Caianiello", Università di Salerno, I-84084 Fisciano, Salerno, Italy
- ⁴⁷INFN, Sezione di Napoli, Gruppo Collegato di Salerno, I-80126 Napoli, Italy
- ⁴⁸Universiteit Antwerpen, 2000 Antwerpen, Belgium
- ⁴⁹Università di Roma "La Sapienza", I-00185 Roma, Italy
- ⁵⁰Univ Rennes, CNRS, Institut FOTON - UMR 6082, F-35000 Rennes, France
- ⁵¹Instituto de Física Teórica UAM-CSIC, Universidad Autónoma de Madrid, 28049 Madrid, Spain
- ⁵²INFN, Laboratori Nazionali del Gran Sasso, I-67100 Assergi, Italy
- ⁵³Laboratoire Kastler Brossel, Sorbonne Université, CNRS, ENS-Université PSL, Collège de France, F-75005 Paris, France
- ⁵⁴Astronomical Observatory Warsaw University, 00-478 Warsaw, Poland

- ⁵⁵Università degli Studi di Milano-Bicocca, I-20126 Milano, Italy
- ⁵⁶INFN, Sezione di Milano-Bicocca, I-20126 Milano, Italy
- ⁵⁷L2IT, Laboratoire des 2 Infinis - Toulouse, Université de Toulouse, CNRS/IN2P3, UPS, F-31062 Toulouse Cedex 9, France
- ⁵⁸Université de Lyon, Université Claude Bernard Lyon 1, CNRS, Institut Lumière Matière, F-69622 Villeurbanne, France
- ⁵⁹Dipartimento di Fisica, Università degli Studi di Genova, I-16146 Genova, Italy
- ⁶⁰INFN, Laboratori Nazionali del Sud, I-95125 Catania, Italy
- ⁶¹Università di Roma Tor Vergata, I-00133 Roma, Italy
- ⁶²INFN, Sezione di Roma Tor Vergata, I-00133 Roma, Italy
- ⁶³Departamento de Astronomía y Astrofísica, Universitat de València, E-46100 Burjassot, València, Spain
- ⁶⁴Dipartimento di Ingegneria Industriale (DIIN), Università di Salerno, I-84084 Fisciano, Salerno, Italy
- ⁶⁵Université Lyon, Université Claude Bernard Lyon 1, CNRS, IP2I Lyon / IN2P3, UMR 5822, F-69622 Villeurbanne, France
- ⁶⁶INAF, Osservatorio Astronomico di Padova, I-35122 Padova, Italy
- ⁶⁷Université libre de Bruxelles, 1050 Bruxelles, Belgium
- ⁶⁸Departamento de Matemáticas, Universitat de València, E-46100 Burjassot, València, Spain
- ⁶⁹Scuola Normale Superiore, I-56126 Pisa, Italy
- ⁷⁰Università degli Studi di Sassari, I-07100 Sassari, Italy
- ⁷¹Dipartimento di Scienze Matematiche, Fisiche e Informatiche, Università di Parma, I-43124 Parma, Italy
- ⁷²INFN, Sezione di Milano Bicocca, Gruppo Collegato di Parma, I-43124 Parma, Italy
- ⁷³Université Lyon, Université Claude Bernard Lyon 1, CNRS, Laboratoire des Matériaux Avancés (LMA), IP2I Lyon / IN2P3, UMR 5822, F-69622 Villeurbanne, France
- ⁷⁴National Center for Nuclear Research, 05-400 Świerk-Otwock, Poland
- ⁷⁵Institut d'Astrophysique de Paris, Sorbonne Université, CNRS, UMR 7095, 75014 Paris, France
- ⁷⁶Université de Strasbourg, CNRS, IPHC UMR 7178, F-67000 Strasbourg, France
- ⁷⁷Institute for Nuclear Research, H-4026 Debrecen, Hungary
- ⁷⁸CNR-SPIN, I-84084 Fisciano, Salerno, Italy
- ⁷⁹Scuola di Ingegneria, Università della Basilicata, I-85100 Potenza, Italy
- ⁸⁰Gravitational Wave Science Project, National Astronomical Observatory of Japan (NAOJ), Mitaka City, Tokyo 181-8588, Japan
- ⁸¹Observatori Astronòmic, Universitat de València, E-46980 Paterna, València, Spain
- ⁸²Centro de Física das Universidades do Minho e do Porto, Universidade do Minho, PT-4710-057 Braga, Portugal
- ⁸³INAF, Osservatorio Astronomico di Capodimonte, I-80131 Napoli, Italy
- ⁸⁴Université de Normandie, ENSICAEN, UNICAEN, CNRS/IN2P3, LPC Caen, F-14000 Caen, France
- ⁸⁵Laboratoire de Physique Corpusculaire Caen, 6 boulevard du maréchal Juin, F-14050 Caen, France
- ⁸⁶Niels Bohr Institute, Copenhagen University, 2100 København, Denmark
- ⁸⁷Department of Physics, Aristotle University of Thessaloniki, 54124 Thessaloniki, Greece
- ⁸⁸University of Białystok, 15-424 Białystok, Poland
- ⁸⁹Institute for High-Energy Physics, University of Amsterdam, 1098 XH Amsterdam, Netherlands
- ⁹⁰Institute of Mathematics, Polish Academy of Sciences, 00656 Warsaw, Poland
- ⁹¹Université Côte d'Azur, Observatoire Côte d'Azur, CNRS, Lagrange, F-06304 Nice, France
- ⁹²NAVIER, École des Ponts, Univ Gustave Eiffel, CNRS, Marne-la-Vallée, France
- ⁹³Università di Firenze, Sesto Fiorentino I-50019, Italy
- ⁹⁴INFN, Sezione di Roma Tre, I-00146 Roma, Italy
- ⁹⁵ESPCI, CNRS, F-75005 Paris, France
- ⁹⁶School of Physics Science and Engineering, Tongji University, Shanghai 200092, China
- ⁹⁷Institut d'Estudis Espacials de Catalunya, c. Gran Capità, 2-4, 08034 Barcelona, Spain
- ⁹⁸Dipartimento di Fisica, Università di Trieste, I-34127 Trieste, Italy
- ⁹⁹Institut des Hautes Etudes Scientifiques, F-91440 Bures-sur-Yvette, France
- ¹⁰⁰Centre national de la recherche scientifique, 75016 Paris, France

- ¹⁰¹Laboratoire Univers et Théories, Observatoire de Paris, 92190 Meudon, France
¹⁰²Observatoire de Paris, 75014 Paris, France
¹⁰³Université PSL, 75006 Paris, France
¹⁰⁴Université de Paris, 75006 Paris, France
¹⁰⁵Consiglio Nazionale delle Ricerche - Istituto dei Sistemi Complessi, I-00185 Roma, Italy
¹⁰⁶Museo Storico della Fisica e Centro Studi e Ricerche “Enrico Fermi”, I-00184 Roma, Italy
¹⁰⁷Dipartimento di Matematica e Fisica, Università degli Studi Roma Tre, I-00146 Roma, Italy
¹⁰⁸Università di Trento, Dipartimento di Matematica, I-38123 Povo, Trento, Italy
¹⁰⁹Subatech, CNRS/IN2P3 - Institut Mines-Telecom Atlantique - Université de Nantes, 4 rue Alfred Kastler BP 20722 44307 Nantes C’EDEX 03, France
¹¹⁰INAF, Osservatorio Astronomico di Brera sede di Merate, I-23807 Merate, Lecco, Italy
¹¹¹Departamento de Matemática da Universidade de Aveiro and Centre for Research and Development in Mathematics and Applications, 3810-183 Aveiro, Portugal
¹¹²Laboratoire MSME, Cité Descartes, 5 Boulevard Descartes, Champs-sur-Marne, 77454 Marne-la-Vallée Cedex 2, France
¹¹³INAF, Osservatorio Astrofisico di Arcetri, I-50125 Firenze, Italy
¹¹⁴Istituto di Astrofisica e Planetologia Spaziali di Roma, 00133 Roma, Italy
¹¹⁵Dipartimento di Scienze Aziendali - Management and Innovation Systems (DISA-MIS), Università di Salerno, I-84084 Fisciano, Salerno, Italy
¹¹⁶Van Swinderen Institute for Particle Physics and Gravity, University of Groningen, 9747 AG Groningen, Netherlands
¹¹⁷Vrije Universiteit Brussel, 1050 Brussel, Belgium
¹¹⁸Eindhoven University of Technology, 5600 MB Eindhoven, Netherlands
- E-mail: maddalena.mantovani@ego-gw.it

Abstract.

The gravitational wave detector Advanced Virgo+ is currently in the commissioning phase in view of the fourth Observing Run (O4).

The major upgrades with respect to the Advanced Virgo configuration are the implementation of an additional recycling cavity, the Signal Recycling cavity (SRC), at the output of the interferometer to broaden the sensitivity band and the Frequency Dependent Squeezing (FDS) to reduce quantum noise at all frequencies.

The main difference of the Advanced Virgo + detector with respect to the LIGO detectors is the presence of marginally stable recycling cavities, with respect to the stable recycling cavities present in the LIGO detectors, which increases the difficulties in controlling the interferometer in presence of defects (both thermal and cold defects).

This work will focus on the interferometer commissioning, highlighting the control challenges to maintain the detector in the working point which maximizes the sensitivity and the duty cycle for scientific data taking.

1. Introduction

The Advanced Virgo detector is a long scale enhanced Michelson interferometer located in Italy, close to Pisa, with the aim of detecting gravitational waves from astronomical sources. The Advanced Virgo interferometer has detected, together with the LIGO interferometers located in the USA [1], an impressive collection of gravitational wave emissions in the last observation runs O2 and O3.

Indeed, during the O2 observation run, just after the joining of the Advanced Virgo detector to the gravitational wave network, the first triple coincidence was observed (GW170817,[2]). During the last observation run (O3), which lasted about one year of data taking from April 2019 to March 2020, about 80 gravitational waves were detected.

After the O3 observation run the Advanced Virgo detector has been upgraded to the Advanced Virgo+ configuration to further improve the sensitivity and join the foreseen O4 run, together

with the LIGO and Kagra detectors, which will start in March 2023.

The major upgrades with respect to the Advanced Virgo detector are:

- Increase of the input power
- Implementation of the Frequency Dependent Squeezing (FDS)
- Addition of the Signal Recycling cavity (SRC).

All the aforementioned upgrades are meant to improve the detector sensitivity, but lead to an increase of complexity in the commissioning of the detector.

The increase of input power will improve the quantum noise at high frequency (shot-noise), but it will also lead to an increase of thermal aberration and radiation pressure effects. The implementation of the FDS will improve the broad-band sensitivity but it requires the installation and commissioning of a completely new hardware system [3]. The addition of the SRC will enhance the detector response to the gravitational wave signal. However it will require to control an additional degree of freedom (both in the longitudinal and angular directions) forcing to completely re-design the lock acquisition scheme and the steady state control scheme. The paper will focus on the commissioning of the Advanced Virgo+ detector upgrades, while the status of the FDS will be detailed in [4].

2. Advanced Virgo+ upgrades

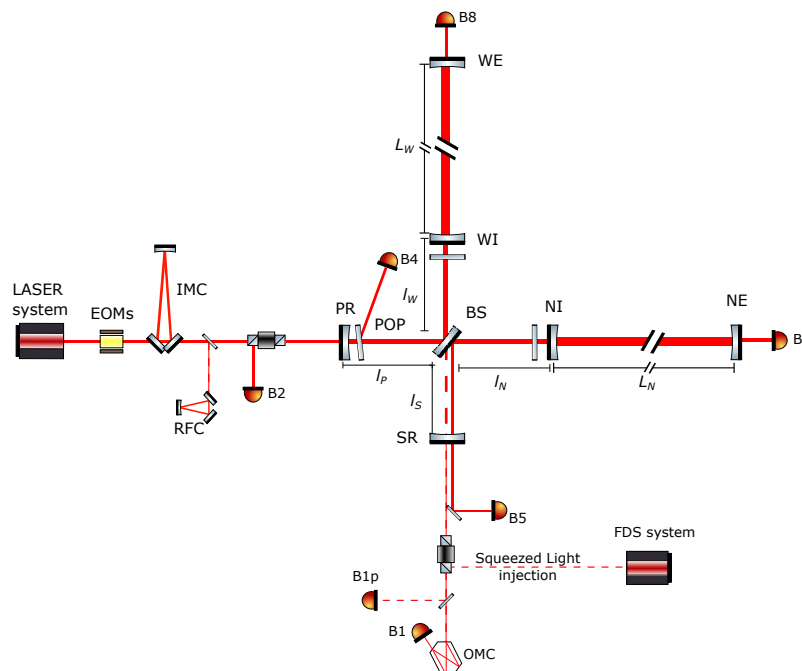


Figure 1. Optical scheme of Advanced Virgo+ in which the main optical components are shown and the main output ports are detailed (B_{XX}). Moreover the Injection system, including the Input Mode Cleaner cavity (IMC) is shown, as well as the Detection system, including the Output Mode Cleaner cavity (OMC). Moreover the FDS system injection point is shown.

The Advanced Virgo+ detector scheme is shown in Figure 1. The input beam is generated by a system of master/slave lasers with a current output power of 33 W after having passed through a 144 m long triangular cavity (Input Mode cleaner, IMC). The main beam is split at the beam splitter mirror (BS) into two beams which are injected into the two orthogonal

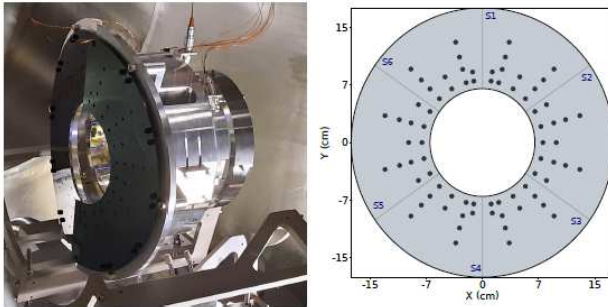


Figure 2. *left* Picture of the instrumented baffle installed in front of MC mirror. *right* Scheme of the embedded diodes on the baffle.



Figure 3. View of the filter cavity for the Frequency Dependent Squeezing.

Fabry-Perot arm cavities (North and West arms), to enhance the phase shift produced by the optical path length variation of the beam caused by a gravitational wave.

The power circulating is enhanced by the Power Recycling, while the SR cavity enhances the response of the detector versus the gravitational wave signal (detected on the dark port B1, see Figure 1). The installation of Advanced Virgo+ has been successfully completed in December 2020.

The major upgrades are the improvement of the injection system, the installation of the Frequency Dependent Squeezing (FDS) and the installation of the SR mirror at the output of the interferometer.

The injection system has been upgraded in order to allow an injected power to the interferometer of 40 W maximum (as a reference the injected power in O3 was 23 W). Moreover the MC mirror payload mechanics has been modified in order to fix controllability issues in the pitch direction, and stray light monitoring has been implemented using a baffle with embedded sensors, see Figure 2 [5].

The baseline design of AdV + involves injecting a Frequency-Dependent Squeezed vacuum field (FDS) in the interferometer (ITF) anti-symmetric port. This should lead to a decrease in the quantum noise contribution over the entire detection bandwidth. The selected method to realize FDS [6] is by exploiting the dispersion in reflection of a frequency independent squeezed (FIS) beam [7] by a detuned 285 meters long filter cavity (FC). The installation of the filter cavity including the 5 additional optical benches (two of which are suspended and operating in vacuum) used for the FC control and FDS injection [8] was completed in March 2021. Afterwards the commissioning phase of the FDS source started. Currently the rotation of the squeezing ellipse at about 20 Hz has been demonstrated with a FC lock accuracy down to 1 Hz and a level of round trip losses lower than 31 ppm in the best condition. These values together with the estimate of the optical propagation losses of 5-6 % and the squeezing ellipse angular jitter of 20 mrad are compliant with the first phase of the project. The second phase of the project, the injection of FDS into the interferometer, has just begun. The FDS cavity external view is shown in Figure 3.

Last but not least, the SR mirror has been added at the dark port of the interferometer. This upgrade is the one that improves the most the target sensitivity but also the one that requires the largest commissioning time since it strongly modifies the optomechanical response of the detector.

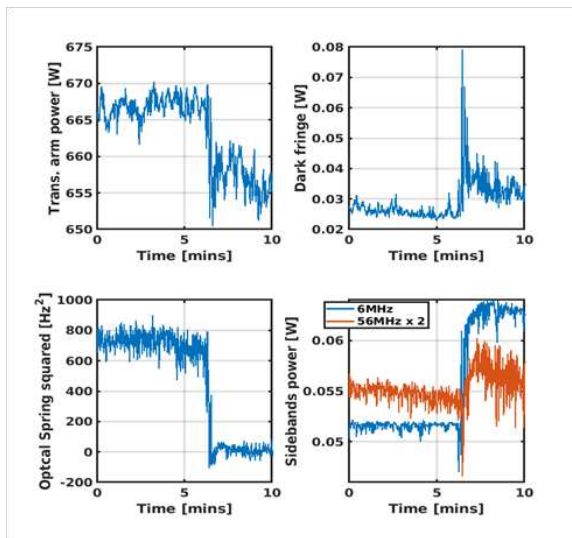


Figure 4. Example of sudden change of state in the detector working point. The change of state is visible in the powers detected in the various ports of the detectors.

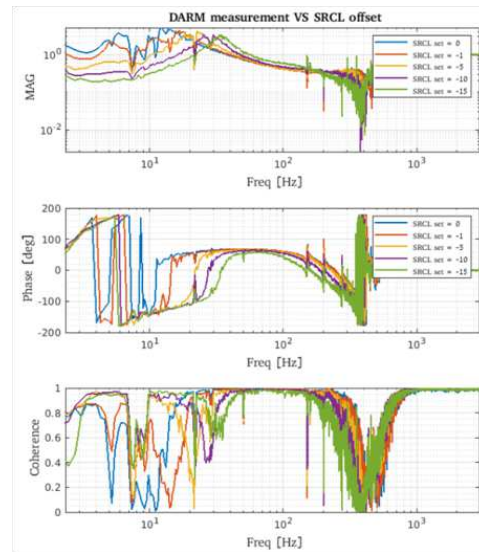


Figure 5. Example of detector response with respect to the SRC working point. It is visible that the structure at low frequency is largely changing the frequency of the peak from 15 Hz to 40 Hz, creating control instabilities.

3. Advanced Virgo+ commissioning phase

After the installation phase, the commissioning of the detector has started in January 2020. As already mentioned, the main part of the commissioning has been devoted to the control of the new optical configuration, including the process which brings the main optical components from the un-controlled state to the precise microscopic positions, called lock acquisition. The set of precise microscopic positions, called working point, is chosen in order to fulfill the resonance conditions of the optical cavities to provide the best sensitivity of the detector.

The control is done based on the Pound-Drever-Hall technique [9], for longitudinal control, and on the Ward technique [10], for the angular control, by adding phase modulations to the main beam (carrier). The phase modulations at 6.27 MHz, 56.44 MHz and 8.36 MHz are realized using Electro-Optic Modulators (EOMs, see Figure 1). The resonance conditions for the modulation sidebands and the Carrier fields, which define the longitudinal working point, are:

- Carrier resonant in the long arm cavities and in the PRC
- 8 MHz sidebands not resonant in any cavity
- 6 MHz sidebands resonant in the PR cavity
- 56 MHz sidebands resonant in the PR and SR cavities

Moreover the differential short Michelson degree of freedom (called MICH, equivalent to $l_n - l_w$) has to be kept in destructive interference.

Due to the addition of the SRC the lock acquisition has been strongly changed with respect to the one developed and implemented for the Advanced Virgo detector [11]. The lock acquisition strategy is generally based on the principle of controlling at first simple configurations and then increase the complexity of the system in semi-adiabatic steps. The lock acquisition developed

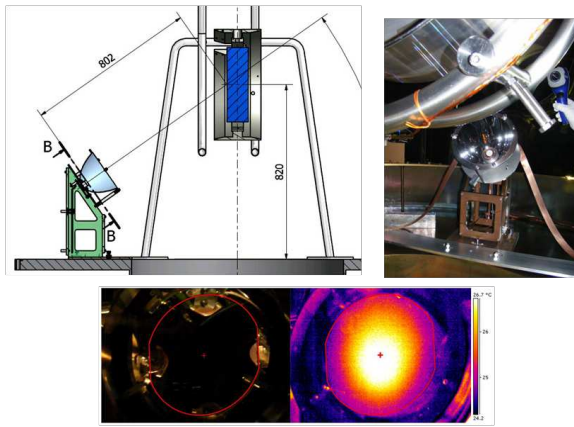


Figure 6. **top left** Technical drawing of the CHRoCC installation. **top right** Picture of the CHRoCC installed in the PR tower **bottom** Picture of the heating profile using, on the right, a thermal camera.

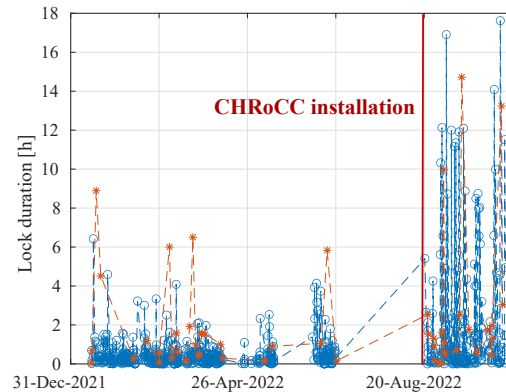


Figure 7. Distribution of the lock duration in hours since the beginning of the commissioning of the detector in the final working point (the red starred locks are the one manually ended). The red line show the start of the locking activities after the installation and pre-commissioning of the CHRoCC.

in Advanced Virgo+ is based on the lock procedure implemented in LIGO which implies the use of auxiliary lasers to disentangle the long arm degrees of freedom from the central area ones, [12] [13] [14] [15].

The first lock at the final working point, described above, with an input power of 33 W has been achieved on December 2021, but the lock showed strong instabilities and un-expected modifications in the detector response. An example of instability is shown in Figure 4, where is visible a sudden change of state in the longitudinal working point which causes lock loss, the so called *jumps*. The other un-expected effect is the strong modification in the opto-mechanical response of the detector. Figure 5 shows an example of the detector response versus the longitudinal position of the SR cavity (SRC set point).

These observations led to strong efforts in simulation studies to understand the origin of the instabilities. The outcomes of the studies proved that a possible cause of the issues was linked to aberrations in the optical configurations. It has to be noted that similar effects have been observed also in LIGO, but with a much lower impact [16]. This can be linked to the fact that Advanced Virgo+, in contrast to the LIGO design, has marginally stable recycling cavities.

The stability of a cavity is a very important characteristic, which depends only on the cavity geometry, and it determines the capability of a cavity to clean and suppress the transverse modes (High Order Modes [17]) generated by optical aberrations. This means that the Advanced Virgo+ detector is much more affected by cold and thermal aberrations with respect to the LIGO detector.

The most affecting parameter has been found to be the PR mirror radius of curvature (RoC) [18], and indeed in the initial optical configuration we had a PR RoC mistuned by 40m (it was pre-tuned to be compliant the thermal configuration of the PRC in case of 125 W of input power) making the PRC unstable. Unfortunately the actuator that was meant to tune the RoC could not be used due to installation problems. This issue has been overcome by adding an additional thermal actuator, called CHRoCC (Central Heating Radius of Curvature Correction, developed in 2013 for initial Virgo [19]). This actuator, visible in Figure 6, has been installed in July 2022

and its working principle is to shine black body radiation to the pick-off plate (POP) placed in front of the PR mirror, see Figure 1, to create a converging lens and to stabilize the PR cavity [20]. After the installation and the pre-commissioning of the actuator the lock stability has been strongly improved.

Figure 7 shows the lock duration distribution from the start of the final working point commissioning (after the complete lock acquisition has been implemented). Moreover it has to be noted that the lock duration distribution is dominated by un-attended operations during nights, since during day time the commissioning activities affect the locking stability.

After the lock losses issue has been mitigated, currently the detector is in the phase of optimizing of the global working point, which includes the tuning of the angular loops and the thermal actuators, to optimize the detector response and achieve good sensitivity for scientific data taking. This phase consists also in the noise hunting campaign to mitigate the technical noise sources and their couplings to the sensitivity.

4. Conclusions

The Advanced Virgo+ detector has successfully concluded the installation phase in 2021 and it is currently in the commissioning phase. The lock acquisition has been completed in December 2021 and a better lock robustness has been achieved after the installation of the CHRoCC actuator. The Advanced Virgo+ commissioning is now entering in the phase of fine tuning of the global working point and in the sensitivity improvement, through a campaign of reduction of technical noise and their coupling to the gravitational wave signal which is called *noise hunting phase*.

References

- [1] Aasi J et al. (LIGO Scientific Collaboration) 2015 *Class. Quant. Grav.* 32 074001
- [2] Abbott B et al. (LIGO Scientific Collaboration, Virgo Collaboration) 2017 *Phys. Rev. Lett.* 119
- [3] Jean-Pierre Zendri, Jean-Francois Cohadon, Fulvio Ricci et al. 'Advanced Virgo Squeezer Technical Design Report' LVK internal note, <https://tds.virgo-gw.eu/ql/?c=11140>, VIR-0411C-15
- [4] The Virgo Collaboration 'Status of Quantum Noise Reduction system in AdV+' proceeding for CRIS 22
- [5] O. Ballester, et. al. 'Measurement of the Stray Light in the Advanced Virgo Input Mode Cleaner Cavity using an instrumented baffle' <https://tds.virgo-gw.eu/ql/?c=17398>, LVC internal note VIR-1149A-21
- [6] H.J.Kimble, Y. Levin Y, A.B.Matsko, K.S.Thorne, S.P. Vyatchanin, *Phys Rev D* 65 022002 (2001)
- [7] M Mehmet and H Vahlbruch, *Class. Quantum Grav.* 36 015014 (2019)
- [8] The Virgo Collaboration, 'Advanced Virgo Plus Phase I Design Report', Virgo-Technical Documentation System, Report No. VIR-0596A-19 (2019) <https://tds.virgo-gw.eu/ql/?c=14430>
- [9] Drever, R.W.P.; Hall, J.L.; Kowalski, F.V.; Hough, J.; Ford, G.M.; Munley, A.J.; Ward, H. 'Laser Phase and Frequency Stabilization 510 Using an Optical Resonator'. *Applied Physics B* 1983, 31, 97–105. <https://doi.org/10.1007/BF00702605>.
- [10] Morrison, E.; Meers, B.J.; Robertson, D.I.; Ward, H. Automatic Alignment of Optical Interferometers. *Applied Optics* 1994, 33, 5041. <https://doi.org/10.1364/AO.33.005041>.
- [11] F. Acernese, et al., 'The variable finesse locking technique, Class'. *Quantum Gravity* 23 (2006) S85–S89
- [12] De Rossi, C.; Brooks, J.; Casanueva Diaz, J.; Chiummo, A.; Genin, E.; Gosselin, M.; Leroy, N.; Mantovani, M.; Montanari, B.; Nocera, F.; Pillant, G. Development of a Frequency Tunable Green Laser Source for Advanced Virgo+ Gravitational Waves Detector. *Galaxies* 2020, 8, 87. <https://doi.org/10.3390/galaxies8040087>
- [13] Staley, A.; Martynov, D.; Abbott, R.; Adhikari, R.X.; Arai, K.; Ballmer, S.; Barsotti, L.; Brooks, A.F.; DeRosa, R.T.; Dwyer, S.; et al. 'Achieving Resonance in the Advanced LIGO Gravitational-Wave Interferometer'. *Classical and Quantum Gravity* 2014, 31, 245010. <https://doi.org/10.1088/0264-9381/31/24/245010>.
- [14] Casanueva Diaz, J.; Leroy, N. 'Auxiliary Laser System: Study of the Lock Acquisition Strategy'. Technical report, Virgo Collaboration, 2019. VIR-0327B-19 <https://tds.virgo-gw.eu/ql/?c=14154>
- [15] D. Bersanetti, M. Boldrini, J. Casanueva Diaz, A. Freise, R. Maggiore, M. Mantovani, M. Valentini 'Simulations for the locking and alignment strategy of the DRMI configuration of the Advanced Virgo+ detector', submitted to *Galaxies MPDI*

- [16] Recording of LIGO-Virgo commissioning meeting, 4 March 2022, <https://dcc.ligo.org/G2200312>
- [17] A.E. Siegman, 'Lasers', University Science Books, Mill Valley, 1986.
- [18] A. C. Green, A. Bianchi, D. D. Brown, A. Freise, R. Maggiore, J. Perry, M. Salle 'Finesse 3 modelling to support AdV+ commissioning to O4: Understanding the DARM Spring (September LVK Talk)' VIR-0875A-22 <https://tds.virgo-gw.eu/ql/?c=18521>
- [19] T Accadia et al 2013 *Class. Quantum Grav.* 30 055017
- [20] A.Chiummo, A. Rocchi, S. Melo, C. De Rossi, E. Capocasa, R. Cavalieri, V. Dattilo, F. Gherardini, J. Degallaix, M. Mantovani, M. Tringali, R. Macchia for the CHRoCC team 'TCS: CHRoCC motivation, preparation and commissioning @VW' Virgo internal document VIR-0696A-22 <https://tds.virgo-gw.eu/ql/?c=18342>